Journal of Biomolecular NMR, 5 (1995) 420–426
ESCOM

J-Bio NMR 286

Selective excitation of intense solvent signals in the presence of radiation damping

Gottfried Otting* and Edvards Liepinsh

Department of Medical Biochemistry and Biophysics, Karolinska Institute, MBB, Doktorsringen 6A, S-171 77 Stockholm, Sweden

Received 17 March 1995
Accepted 19 April 1995

Keywords: Radiation damping; Selective water excitation; Water–protein NOEs; Protein hydration; BPTI; Lysozyme

Summary

Selective water excitation schemes are provided which rely on the radiation damping effect in probeheads characterized by high quality factors. The schemes are implemented in homonuclear NOE and ROE experiments, designed for the selective observation of water–protein cross peaks and their assignment using standard probeheads. The one-dimensional NOE and ROE experiments selectively record the cross section through the water signal usually measured in two-dimensional NOESY and ROESY spectra, and the two-dimensional NOE-NOESY and ROE-NOESY experiments selectively measure the cross section through the water line from 3D NOESY-NOESY and ROESY-NOESY spectra, respectively.

The study of protein hydration by intermolecular ^{1}H-^{1}H NOEs between the water and the protein signals is frequently impeded by weak intensities of the water–protein NOEs and overlap between the water–protein cross peaks. In a two-dimensional NOESY or ROESY experiment, these water–protein cross peaks are observed in a single cross section through the water line, since the rapid chemical exchange between hydration water and bulk water leads to the coalescence of all water proton chemical shifts in a single, average water resonance (Otting et al., 1991a). Consequently, it was proposed to record the cross section of interest directly in a one-dimensional experiment, using a selective pulse for water excitation (Kriwacki et al., 1993; Mori et al., 1994; Qi et al., 1994; Otting and Liepinsh, 1995).

The selective excitation of the water resonance is hampered by the radiation damping effect which is significant in probeheads with high quality factor for signals as intense as the water signal. The present communication shows how radiation damping can be used constructively for the excitation of the water signal.

Radiation damping arises from the interaction of precessing transverse magnetization with the radiofrequency coil (Abragam, 1961). The current induced in the coil acts back on the magnetization like a weak radiofrequency pulse, turning the magnetization back towards its thermal equilibrium position (the z-axis of the magnetic field). Figure 1 demonstrates the effect with simple 1D experiments (β-degree pulse acquisition) using a sample of 90% H_2O/10% D_2O. The carrier was set at the water frequency and the receiver phase was adjusted so that the signal appeared only in one of the two quadrature channels. Four FIDs of the ^{1}H NMR resonance of the water signal, observed after pulses of different flip angles β, are shown in superposition. The leftmost trace shows the FID after a 90° pulse. Because of radiation damping, the FID decays much faster than expected for the T_2 relaxation time of water, which is longer than 1 s. After a 170° pulse (second trace from the left), the small transverse component of the magnetization is sufficient to initiate radiation damping, which turns the magnetization through the transverse plane back to the z-axis. Even after a 180° pulse (third trace from the left), enough transverse magnetization is present to initiate the radiation damping effect after a few milliseconds. If the 180° pulse is followed by a pulsed field gradient of 2 ms duration, the magnetization remains aligned along the negative z-axis for a longer time period because the transverse magnetization is defocussed over the sample. This effect has been exploited earlier by Guéron and co-workers for T_1 relax-

*To whom correspondence should be addressed.

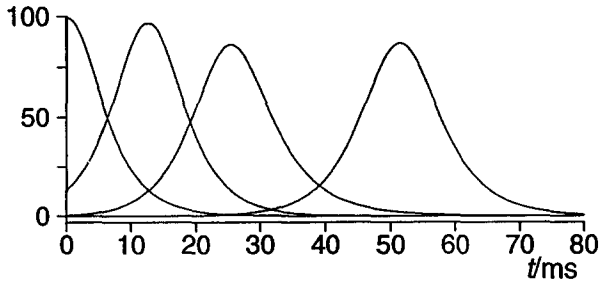

Fig. 1. Superposition of four experimental FIDs, illustrating the effect of radiation damping. The FIDs were recorded at a ^1H frequency of 600 MHz using a sample of 90% H_2O / 10% D_2O. The carrier was set on-resonance of the water proton signal. The phase of the excitation pulse was adjusted for each FID, so that the entire signal was recorded in only one of the two quadrature detection channels. The leftmost FID was obtained after a 90° pulse, the following two FIDs were obtained after a 170° and a 180° pulse, respectively, and the rightmost FID is the result of a 180° pulse, followed by a z-gradient pulse of 2 ms duration applied to the room temperature shim system (homospoil). The vertical scale was adjusted by attributing a value of 100 to the signal intensity observed for fully transverse magnetization.

ation measurements of the water signal (Leroy et al., 1985). Yet, after some time transverse magnetization builds up and the magnetization is turned back to the positive z-axis by radiation damping (rightmost trace). In the latter two cases, the phase of the transverse magnetization which is generated by the radiation damping effect varies from scan to scan in a practically random manner. However, the transverse magnetization generated by a 170° or, better, 160° pulse, is sufficient to initiate radiation damping with a predictable phase.

The maximum strength of the radiation damping field can be estimated from the speed with which the magnetization passes through the transverse plane (Fig. 1) to be between 25 and 30 Hz. Any selective excitation scheme using a shaped pulse would have to overcome this field strength to achieve an effective 90° or 180° rotation of the water signal. This excludes the use of long, very selective pulses. Much more selective pulses can be generated if the current induced in the rf-coil by radiation damping itself is used to excite the water signal. The effective pulse shapes are given by the FIDs displayed in Fig. 1. They are reminiscent of a Gaussian function, which has been shown to give very favourable excitation profiles (Bauer et al., 1984).

Two principally different schemes are conceivable which use radiation damping for selective excitation. (i) The radiation damping following the incomplete inversion by a nonselective 160° pulse is used. After about 30 ms, most of the water magnetization has returned to the positive z-axis (Fig. 1, second trace) while the solute resonances off-resonance from the solvent signal do not experience the radiation damping effect. Subtracting a spectrum without radiation damping yields the selectively inverted water line. The radiation damping may be suppressed using either pulsed field gradients (homospoil pulses) after

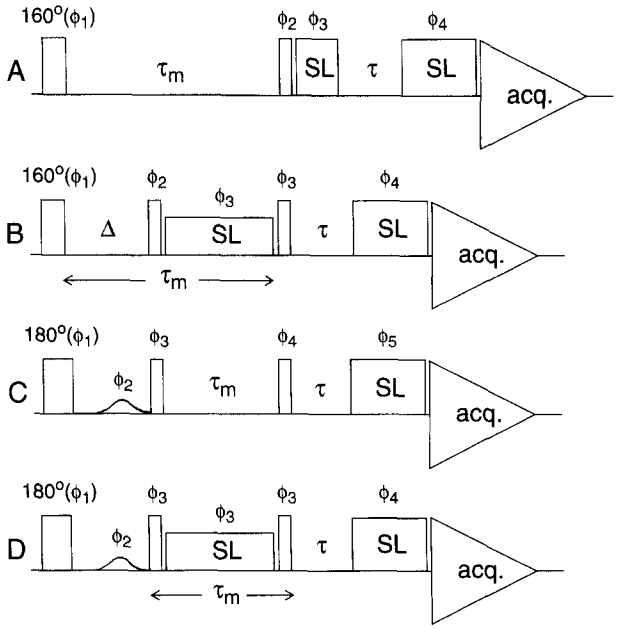

Fig. 2. Experimental schemes for one-dimensional NOE and ROE experiments with selective water excitation. All pulses are nonselective, except for a shaped pulse in schemes C and D. Narrow bars denote 90° pulses, wider bars denote 160° and 180° pulses, and spin-lock pulses are labelled SL. The water signal is suppressed in all experiments by a short free precession delay τ and a spin-lock pulse of about 2 ms duration (Otting et al., 1991c,1992). The resulting excitation profile depends with $\sin(\Omega\tau)$ on the angular frequency Ω relative to the carrier (Otting et al., 1991c). Schemes A and B are difference experiments, where the signal from a scan recorded with homospoil pulses after the 160° pulse is subtracted from the signal of an otherwise identical scan without homospoil pulses. The mixing time τ_m of the 1D NOE experiment (A) and the delay Δ in the 1D ROE experiment (B) must be chosen sufficiently long to allow a complete return of the water magnetization to the positive z-axis by radiation damping. Radiation damping is suppressed in the experiments with homospoil pulses. In the 1D NOE experiment (A), the homospoil pulses are repeated at regular intervals throughout the mixing time τ_m to prevent radiation damping. In schemes C and D, a 2 ms homospoil pulse following the 180° excitation pulse retains the magnetization aligned along the negative z-axis for about 30 ms. A selective pulse with a very small nominal flip angle is applied to the water resonance to trigger radiation damping after the homospoil pulse and a short delay for the recovery of the homogeneity of the magnetic field. The amplitude of the selective pulse is adjusted so that the water magnetization is transverse at the end of the selective pulse. The following 90° pulse in the 1D NOE experiment (C) generates longitudinal water magnetization. Homospoil pulses applied during the following mixing time τ_m suppress radiation damping. In the 1D ROE pulse sequence (D), the transverse water magnetization is spin-locked for ROESY mixing. The mixing period is flanked by two 90° pulses for off-resonance compensation (Griesinger and Ernst, 1987). Phase cycling: (A) $\phi_1 = 4(x,-x)$, $\phi_2 = 2(x,x,-x,-x)$, $\phi_3 = 8(y)$, $\phi_4 = 4(x),4(-x)$, receiver = 2(x,x,−x,−x); (B) $\phi_1 = 8(x,-x)$, $\phi_2 = 4(x,x,-x,-x)$, $\phi_3 = 2(y,y,y,y,-y,-y,-y,-y)$, $\phi_4 = 8(x),8(-x)$, receiver = 4(x,x,−x,−x); (C) $\phi_1 = 16(x,-x)$, $\phi_2 = 8(x,x,-x,-x)$, $\phi_3 = 4(x,x,x,x,-x,-x,-x,-x)$, $\phi_4 = 8(x),8(-x),8(x),8(-x)$, $\phi_5 = 16(x),16(-x)$, receiver = 2[2(x),4(−x),2(x),2(−x),4(x),2(−x)]; (D) same as (B). Each phase cycle is extended fourfold by the use of CYCLOPS (Hoult and Richards, 1975).

the 160° pulse to defocus any transverse magnetization which could induce radiation damping (Leroy et al., 1985), or by switching the Q-factor of the rf-coil to a low

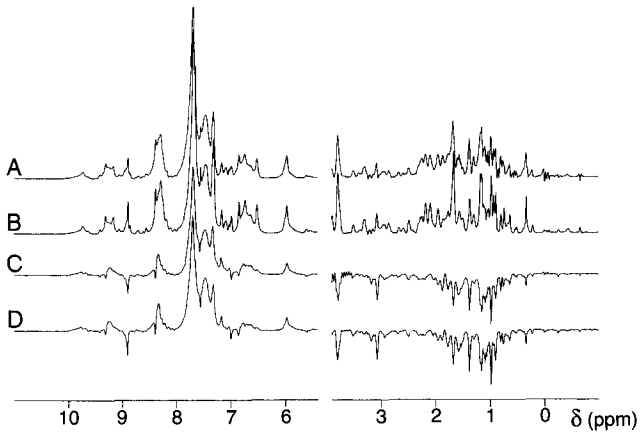

Fig. 3. Comparison between water–protein cross peaks recorded with the 1D NOE and ROE experiments of Figs. 2A and B and the corresponding cross sections through 2D NOESY and ROESY spectra. The data were recorded using a 10 mM solution of lysozyme in 90% H_2O/10% D_2O at pH = 3.8 and 36 °C. The relaxation agent Gd(DTPA–BMA) was added at a final concentration of 0.75 mM to shorten the T_1 relaxation time of the water signal to about 0.45 s (Otting and Liepinsh, 1995). The same water suppression technique was used in all spectra, setting the carrier at the water frequency and suppressing the water signal by a spin-lock pulse of 2 ms, following a delay τ of 100 μs (Otting et al., 1991c). For improved presentation, the sign change of the excitation profile at the water frequency was compensated by inverting the low-field halves of the spectra before plotting. In addition, the spectral region between −1 and 4 ppm was plotted on a four times larger scale, because the exchange peaks in the region 5.5 to 11 ppm were much more intense than the cross peaks in the high-field region. Homospoil pulses were of 2 ms duration, with sine-bell amplitudes, and were applied to the room temperature z-shim coil using the standard equipment and software provided by the manufacturer. All spectra were recorded using the same acquisition parameters, with a relaxation delay between subsequent scans of about 1.1 s. Baseline corrections were performed in all dimensions using polynomials. (A) 1D NOE spectrum recorded with the pulse sequence of Fig. 2A. Experimental parameters: $\tau_m = 60$ ms, duration of the first spin-lock pulse 500 μs, total experimental time about 45 min. Two homospoil pulses were used during the mixing time at an interval of 28 ms. (B) Cross section through a 2D NOESY spectrum taken along the δ_2 chemical shift axis at the δ_1 chemical shift of the water signal. The spectrum was recorded with the pulse sequence described by Otting et al. (1992) using the same mixing time and water suppression technique as in (A), except for the omission of the first spin-lock pulse. $t_{1max} = 59$ ms, total recording time 6 h. (C) 1D ROE spectrum recorded with the pulse sequence of Fig. 2B. The ROESY mixing spin-lock consisted of a series of 30° pulses, separated by 17 μs delays for a duration of 40 ms (Kessler et al., 1987). $\Delta = 30$ ms, total recording time about 45 min. (D) Cross section through a 2D ROESY spectrum taken along the δ_2 chemical shift axis at the δ_1 chemical shift of the water signal. The spectrum was recorded with the pulse sequence described by Otting et al. (1991c) using a mixing time of 30 ms and the same t_{1max} value and total recording time as in (B). The spectra were recorded at 600 MHz ^1H frequency on a Bruker AMX-2 600 NMR spectrometer.

value (Anklin et al., 1995). (ii) A pulsed field gradient is applied after a nonselective 180° inversion pulse. Without further pulses, the magnetization would remain along the −z-axis for about 30 ms (Fig. 1, rightmost trace). Using a very weak and selective shaped pulse, a transverse component of the magnetization is generated, thus triggering radiation damping in a reproducible way. The amplitude of the selective pulse is adjusted so that the water magnetization arrives in the transverse plane after about 25 ms. Opposite phases of the shaped pulse yield opposite phases of the transverse water magnetization. The resulting excitation corresponds to a selective 90° pulse, applied to the water signal with a shape described by the first half of the third trace in Fig. 1, which is reminiscent of a half-Gaussian pulse (Friedrich et al., 1987).

Since scheme (i) corresponds to a selective inversion pulse, its excitation profile is narrower than the effective 90° pulse of scheme (ii) (Boudot et al., 1989). Furthermore, scheme (i) proved to be more sensitive by about a factor $\sqrt{2}$, apparently because not all water magnetization arrives in the transverse plane simultaneously and with exactly the same phase in scheme (ii). However, scheme (ii) is less prone to subtraction artefacts, since here the selection of the water signal is based on the phase of a very weak and selective pulse, whereas scheme (i) takes the difference between two scans recorded with a different number of gradients and therefore different amounts of eddy currents present during the excitation sequence. In mixed solvents with more than one intense solvent signal, scheme (ii) can be used to excite any of the solvent signals in a selective way.

Figure 2 shows implementations of schemes (i) and (ii) in pulse sequences designed for the observation of water–protein NOEs in one-dimensional NOE and ROE spectra. In all pulse sequences, the water signal is suppressed immediately before signal detection by a free precession delay τ and a spin-lock pulse (Otting et al., 1991c), but, if self-shielded gradients are available, schemes like WATERGATE (Piotto et al., 1992) can also be used. The use of spin-lock pulses has the advantage that the experiments can be performed on any probehead without gradient coil. All pulsed field gradients used in the excitation schemes are followed by relatively long delays, during which the magnetic field homogeneity can recover after application of gradient pulses to the room temperature z-shim coil. On our NMR spectrometer, sine-shaped gradients of 2 ms, applied every 20 ms with a maximum amplitude of about 0.5 G/cm, were found to be sufficient for the suppression of radiation damping and the eddy currents were negligible 18 ms after the gradient pulse.

Figure 2A shows scheme (i), implemented in a 1D NOE experiment. After the 160° pulse, the water magnetization returns to the positive z-axis during the mixing time by radiation damping, while radiation damping is suppressed in a corresponding experiment with gradient pulses applied every 20 ms during the mixing time. The mixing time must be chosen sufficiently long to allow for nearly complete return of the water magnetization in those scans where radiation damping is active. The effective mixing time for the transfer of water magnetization to protein protons is different for scans with and without

suppression of radiation damping: it corresponds to τ_m with the radiation damping suppressed, but is shorter in the presence of radiation damping because the sign and size of the longitudinal magnetization transferred by the NOE change as the water magnetization passes through the transverse plane on its way back to the positive z-axis.

Figure 2B shows the corresponding scheme for a 1D ROE experiment. The delay Δ is chosen as short as possible, in order to selectively invert the water signal without generating too much NOE between water and protein. The subsequent 90° pulse brings the water magnetization back into the transverse plane, where it is spin-locked. The spin-lock pulse is followed by an off-resonance compensating 90° pulse (Griesinger and Ernst, 1987). For dipolar interactions in the slow motional regime, the ROE in this experiment is counteracted by the NOE building up during the excitation delay Δ. To reduce the importance of the NOE, the ROE spin-lock should be chosen longer than the excitation period Δ (Fig. 2B). Similar to the 1D NOE experiment (Fig. 2A), the amount of NOE present differs between the experiments with and without suppression of radiation damping.

Figures 2C and D show pulse sequences for 1D NOE and ROE equivalent to those of Figs. 2A and B, except that scheme (ii) is used for the selective excitation of the water signal. Since the water magnetization is transverse at the end of the shaped pulse excitation, a 90° pulse is required to generate longitudinal magnetization at the beginning of the NOE mixing time τ_m (Fig. 2C). In the ROE experiment, the water magnetization is spin-locked immediately after its selective excitation (Fig. 2D). The ROE mixing period is framed by 90° pulses for off-resonance compensation (Griesinger and Ernst, 1987). In contrast to the pulse sequences of Figs. 2A and B, the NOEs building up between the water and the protein protons during the selective excitation scheme are subtracted by the phase cycling of the selective pulse, leading to well-defined NOE and ROE mixing times.

The performance of the selective pulse sequences of Fig. 2 was compared with the aid of the water–protein cross peaks observed in the one-dimensional cross sections through the water signal in two-dimensional NOESY and ROESY spectra of hen egg white lysozyme and bovine pancreatic trypsin inhibitor (BPTI). Figure 3A shows the water–protein NOEs recorded with the 1D NOE experiments of Fig. 2A. The spectrum is virtually identical to the corresponding cross section through the 2D NOESY experiment (Fig. 3B), except for small differences in the high-field region of the spectrum. Similarly, the 1D ROE spectrum (Fig. 3C) recorded with the pulse sequence of Fig. 2B is almost identical to the corresponding cross section through the 2D ROESY experiment (Fig. 3D). Small differences are present for some of the methyl resonances, e.g. near 0 ppm, but the artefacts are fewer and less intense than in the NOE cross section of Fig. 3A. The signal-to-noise ratio of the 1D spectra is comparable to that of the cross sections through the 2D spectra, although they were recorded in much less time (Fig. 3). The 1D experiments thus present most sensitive techniques for the rapid measurement of chemical exchange peaks between water and protein protons. They also reliably detect the intense water–protein NOEs which are typically observed for hydration water molecules in

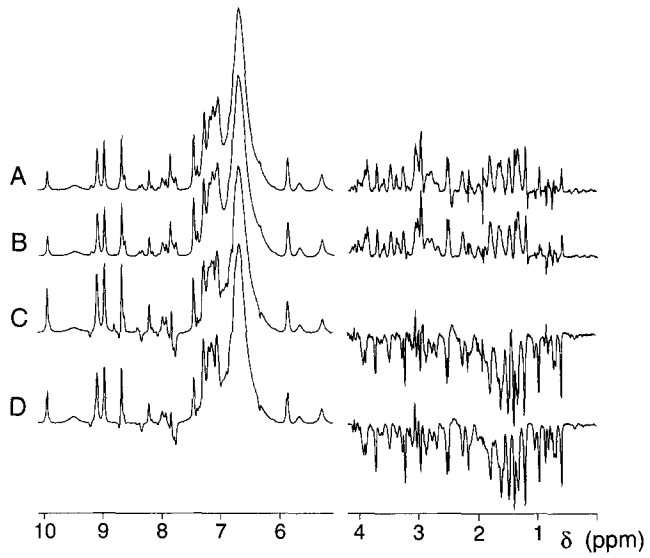

Fig. 4. Comparison between water–protein cross peaks recorded with the 1D NOE and ROE experiments of Figs. 2C and D and the corresponding cross sections through two-dimensional NOESY and ROESY spectra. The data were recorded using a 20 mM solution of BPTI in 90% H_2O/10% D_2O at pH = 6.9 and 36 °C, containing 0.75 mM Gd(DTPA–BMA). The same water suppression technique and homospoil pulse settings were used as in the experiments of Fig. 3, except that the delay τ was set to 127 μs. For improved presentation, the sign change of the excitation profile at the water frequency was compensated by inverting the low-field halves of the spectra before plotting. In addition, the spectral region between 0 and 4 ppm was plotted on an eight times larger scale. All spectra were recorded using the same acquisition time, spectral width and receiver gain. The relaxation delay between subsequent scans was about 1.2 s. Baseline corrections were performed in all dimensions using polynomials. (A) 1D NOE spectrum recorded with the pulse sequence of Fig. 2C. Experimental parameters: $\Delta = 35$ ms, $\tau_m = 50$ ms with two homospoil pulses applied at a 23 ms interval, total experimental time about 1.5 h. The selective pulse was a 25 ms Gaussian pulse applied after a 2 ms homospoil pulse and an 8 ms delay for recovery of the homogeneity of the static magnetic field. The nominal flip angle of the Gaussian pulse was 0.3°. (B) Cross section through a 2D NOESY spectrum taken along the δ_2 chemical shift axis at the δ_1 chemical shift of the water signal. The spectrum was recorded with the pulse sequence described by Otting et al. (1992), using the same mixing time as in (A). $t_{1max} = 61$ ms, total recording time about 6 h. (C) 1D ROE spectrum recorded with the pulse sequence of Fig. 2D. The ROESY mixing spin-lock consisted of a series of 30° pulses, separated by 17 μs delays for a duration of 50 ms (Kessler et al., 1987). The same excitation sequence and total recording time as in (A) were applied. (D) Cross section through a 2D ROESY spectrum taken along the δ_2 chemical shift axis at the δ_1 chemical shift of the water signal. The spectrum was recorded with the pulse sequence described by Otting et al. (1991c), using the same mixing time, t_{1max} value and total recording time as in (B).

the interior of a protein (Otting et al., 1991b). However, weak cross peaks, particularly those from narrow methyl resonances, must be regarded with scepticism because of the presence of artefactual peak intensities in the 1D experiments which do not appear in the 2D NOESY and ROESY experiments. These could be subtraction artefacts, associated with the different number of homospoil pulses used with each of the difference experiments of Figs. 2A and B, since their appearance is not fully reproducible. This view is supported by the fact that the level of artefacts is much lower in experiments using a Q-switched selective pulse for the water excitation (Otting and Liepinsh, 1995) or the experimental schemes of Figs. 2C and D.

The experiments of Figs. 2C and D select the water signal by phase cycling of a selective pulse, rather than by the difference between experiments conducted with and without homospoil pulses. Figure 4A shows the water–protein NOEs recorded with the 1D NOE experiments of Fig. 2C. The spectrum is very similar to the corresponding cross section through the 2D NOESY experiment (Fig. 4B). Similarly, the 1D ROE spectrum (Fig. 4C) recorded with the pulse sequence of Fig. 2D closely reproduces the corresponding cross section through the 2D ROESY experiment (Fig. 4D). Some differences between the 1D experiments and the cross sections through the 2D spectra are observed: sharp spikes, e.g. at about 1.9 ppm, and somewhat different intensities which are most pronounced for the narrow methyl resonances near 0.8 ppm. Narrow line widths and spike intensities seem to correlate in the spectra of Fig. 4, suggesting that the spikes represent subtraction artefacts. The most striking differences come from intra-protein cross peaks with α-proton resonances which are nearly degenerate with the water signal. These include the negative cross peak at about 2.3 ppm in Fig. 4A and the weak positive cross peaks at 8.3 and 8.7 ppm in Fig. 4C, which are different in Fig. 4D. Overall, the selective excitation scheme of Figs. 2C and D reproduces the water–protein cross sections from the two-dimensional spectra more faithfully than the excitation scheme of Figs. 2A and B, at the price of somewhat reduced sensitivity.

The selective excitation schemes of Fig. 2 are readily incorporated into pulse sequences which record the two-dimensional cross sections through the water signal in 3D NOESY-NOESY and ROESY-NOESY experiments as two-dimensional spectra. As in the case of the one-dimensional spectra, the reduction from three to two dimensions is accompanied by increased sensitivity and the possibility to obtain higher spectral resolution in shorter recording times. Figure 5 shows pulse sequences for 2D NOE-NOESY and ROE-NOESY experiments, using selective water excitation schemes based on radiation damping after a 160° pulse (Figs. 5A and B) or radiation damping triggered by a selective 90° pulse (Figs. 5C and D). The pulse schemes are straightforward extensions of the 1D experiments of Fig. 2, using the selectively generated water–protein cross peaks as starting magnetization for conventional NOESY experiments.

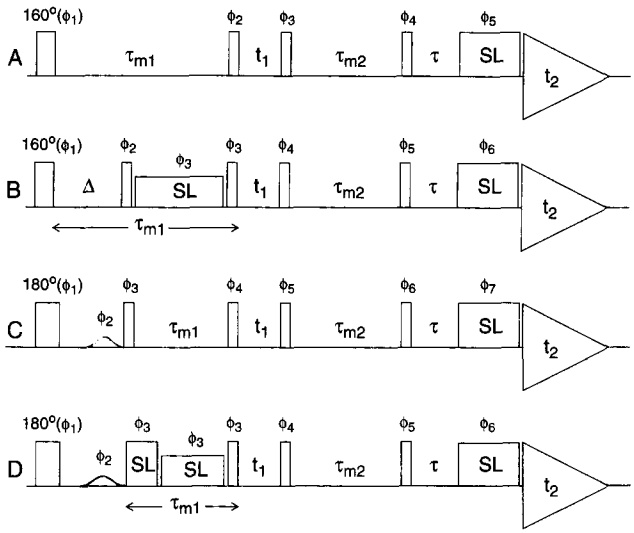

Fig. 5. Experimental schemes for two-dimensional NOE–NOESY and ROE–NOESY experiments with selective water excitation. The water signal is suppressed in the same way as in the experiments of Fig. 2, i.e., by a short free precession delay τ and a spin-lock pulse of 1–2 ms duration (Otting et al., 1991c,1992). (A) and (B): 2D NOE-NOESY and 2D ROE-NOESY sequence, respectively, using the selective excitation scheme of Figs. 2A and B. Homospoil pulses, applied during the second mixing time τ_{m2}, support the coherence order selection and enable water suppression by a single spin-lock pulse (Otting et al., 1992). (C) and (D): 2D NOE-NOESY and 2D ROE-NOESY sequence, respectively, using the selective excitation scheme of Figs. 2C and D. Phase cycling: (A) $\phi_1 = 8(x,-x)$, $\phi_2 = 4(x,x,-x,-x)$, $\phi_3 = 2(x,x,x,x,-x,-x,-x,-x)$, $\phi_4 = 16(x)$, $\phi_5 = 8(x),8(-x)$, receiver = 2(x,x,−x,−x,−x,−x,x,x); (B) $\phi_1 = 16(x,-x)$, $\phi_2 = 8(x,x,-x,-x)$, $\phi_3 = 4(y,y,y,y,-y,-y,-y,-y)$, $\phi_4 = 2[8(x),8(-x)]$, $\phi_5 = 32(x)$, $\phi_6 = 16(x),16(-x)$, receiver = 2[2(x,x,−x,−x),2(−x,−x,x,x)]; (C) $\phi_1 = 8(x,x,-x,-x)$, $\phi_2 = 16(x,-x)$, $\phi_3 = 4(x,x,x,x,-x,-x,-x,-x)$, $\phi_4 = 2[8(x),8(-x)]$, $\phi_5 = \phi_6 = 32(x)$, $\phi_7 = 16(x),16(-x)$, receiver = 2[2(x,−x),4(−x,x),2(x,−x)]; (D) $\phi_1 = 8(x,x,-x,-x)$, $\phi_2 = 16(x,-x)$, $\phi_3 = 4(y,y,y,y,-y,-y,-y,-y)$, $\phi_4 = 2[8(x),8(-x)]$, $\phi_5 = 32(x)$, $\phi_6 = 16(x),16(-x)$, receiver = 2[4(x,−x),4(−x,x)]. The phase cycles may be shortened by omitting the phase cycling of the 90° pulse before τ_{m2}. Because of the coherence order selection associated with spin-lock pulses (Counsell et al., 1985), the phases of the ROE mixing spin-locks in (B) and (D) do not have to be phase cycled. In experiments using mixing times shorter than about 50 ms, the coherence order selection by the spin-lock may be supported by spin-locking at high power for the first 1 to 2 ms, as illustrated in (D). Use of CYCLOPS increases the phase cycles fourfold (Hoult and Richards, 1975). Quadrature detection in the F_1 dimension is achieved by applying TPPI or States-TPPI to all pulses before the evolution time t_1 (Marion and Wüthrich, 1983; Marion et al., 1989).

Figure 6 shows NOE-NOESY and ROE-NOESY spectra of hen egg white lysozyme which were recorded using the pulse sequences of Figs. 5A and B. The interpretation of these spectra is completely analogous to that of the 2D cross sections taken at the water frequency through 3D NOESY-NOESY and ROESY-NOESY spectra (Otting et al., 1991c; Holak et al., 1992). The diagonal peaks are from the protons to which magnetization was transferred,

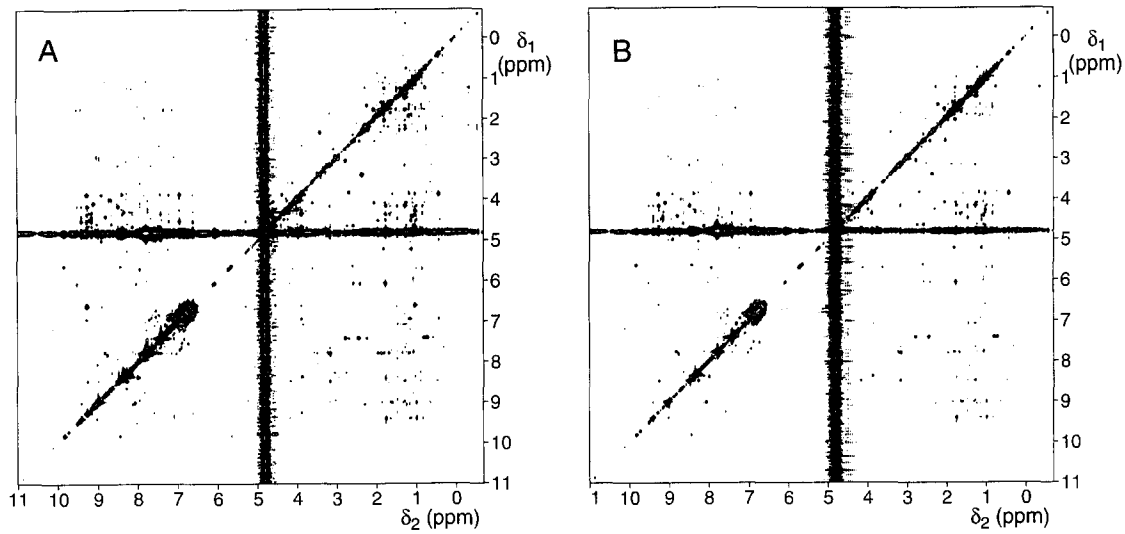

Fig. 6. (A) 2D NOE-NOESY and (B) 2D ROE-NOESY spectra recorded with the experimental schemes of Figs. 5A and B, respectively. The lysozyme sample and solution conditions were identical to those used in Fig. 3. The spectra were recorded in about 45 h each, using a second mixing time τ_{m2} of 90 ms with three homospoil pulses every 28 ms during τ_{m2}. t_{1max} = 46 ms, t_{2max} = 119 ms, relaxation delay between subsequent scans = 1.1 s. The first mixing time τ_{m1} was 60 ms in the NOE-NOESY experiment and 80 ms in the ROE-NOESY experiment with Δ = 40 ms. A 160° pulse was used for the initial excitation. In the scans with suppression of radiation damping, the 160° pulse was followed by two homospoil pulses of 2 ms duration, separated by a delay of 18 ms. The water signal was suppressed by a spin-lock pulse of 2 ms length. The baseline was corrected using polynomials in both dimensions. Positive and negative contour levels are plotted without distinction.

either by chemical exchange or NOE from the water signal during the first mixing time τ_{m1} (Fig. 5). In addition, some of the diagonal peaks may arise from protons interacting with α-protons which resonate at the same chemical shift as the water signal, since the radiofrequency field generated by the radiation damping of the water magnetization acts back not only on the water magnetization itself, but also on any magnetization at the same frequency. The off-diagonal peaks arise from intra-protein NOEs during the second mixing time τ_{m2} and are readily assigned by comparison with a conventional NOESY spectrum. The assignments of the δ_1 chemical shifts of the off-diagonal peaks identify the protons interacting with water. The cross section along the δ_2 chemical shift axis at the δ_1 chemical shift of the water signal in Fig. 6 contains the signals arising from magnetization transfer pathways which start from water magnetization, precess with the water frequency during t_1, and are transferred to protein protons during the second mixing time τ_{m2}. This cross section contains the same information as the conventional cross sections shown in Figs. 3A and B and includes those chemical exchange peaks which are not present as diagonal peaks in Fig. 6 because they relax too rapidly by fast proton exchange with the water.

Experiments using a Q-switched pulse for selective water excitation seem to be least troubled by artefacts (Otting and Liepinsh, 1995). However, using a 160° pulse combined with radiation damping provides the most sensitive selective water excitation technique. Although the signal-to-noise ratio observed in the cross sections through the 2D NOESY and ROESY spectra in Figs. 3 and 4 could have been improved significantly by the use of B_1 gradients (Otting, 1994) or a probehead with Q-switch (Anklin et al., 1995), the selective one-dimensional experiments are always intrinsically more sensitive. All selective water excitation schemes presented here can be used with regular selective proton probeheads, which tend to have better signal-to-noise characteristics than probeheads equipped with gradient coils. The selectivity of the water excitation by radiation damping depends strongly on the magnetic field strength, since the voltage induced in the radiofrequency coil by the precessing water magnetization is proportional to the magnetization of the sample and the frequency (Abragam, 1961). In practice, we find that the excitation scheme of Figs. 2A and B is ineffective at a proton frequency of 400 MHz, whereas the scheme of Figs. 2C and D is still viable with an increased amplitude of the selective pulse. At much higher frequencies than 600 MHz, the selectivity of either of the two excitation schemes will be compromised by too rapid radiation damping.

Independent of the water excitation scheme used, the sensitivity in the NOE-NOESY and ROE-NOESY experiments of Fig. 5 can be improved further by using water suppression schemes with more uniform excitation profiles in the detection dimension. For example, the combination of a selective 90° pulse on the water signal, followed by a nonselective 90° pulse of opposite phase (Sklenář et al., 1987), can be used for the final signal readout instead of spin-lock pulses, provided that the water magnetization is aligned along the positive z-axis by the end of the second mixing time τ_{m2}. This is readily

achieved by radiation damping, if τ_{m2} is sufficiently long and no homospoil pulses are applied during this mixing period. The radiation damping may be supported by phase shifting the 90° pulse that precedes the mixing time by 45° with respect to all other pulses (Jahnke et al., 1995).

The improved sensitivity of the experiments presented here will extend the range of proteins for which hydration can be studied on the molecular level by the measurement of water–protein NOEs.

Acknowledgements

Financial support from the Swedish Natural Science Research Council (project 10161) and the Wallenberg Foundation is gratefully acknowledged.

References

Abragam, A. (1961) *Principles of Nuclear Magnetism*, Clarendon Press, Oxford.

Anklin, C., Rindlisbacher, M., Otting, G. and Laukien, F.H. (1995) *J. Magn. Reson. Ser. B*, **106**, 199–201.

Bauer, C., Freeman, R., Frenkiel, T., Keeler, J. and Shaka, A.J. (1984) *J. Magn. Reson.*, **58**, 442–457.

Boudot, D., Canet, D., Bondeau, J. and Boubel, J.C. (1989) *J. Magn. Reson.*, **83**, 428–439.

Counsell, C.J.R., Levitt, M.H. and Ernst, R.R. (1985) *J. Magn. Reson.*, **64**, 470–478.

Friedrich, J., Davis, S. and Freeman, R. (1987) *J. Magn. Reson.*, **75**, 390–395.

Griesinger, C. and Ernst, R.R. (1987) *J. Magn. Reson.*, **75**, 261–271.

Holak, T.A., Wiltcheck, R. and Ross, A. (1992) *J. Magn. Reson.*, **97**, 632–636.

Hoult, D. and Richards, R.E. (1975) *Proc. R. Soc. London Ser. A*, **344**, 311–340.

Jahnke, W., Baur, M., Gemmecker, G. and Kessler, H. (1995) *J. Magn. Reson. Ser. B*, **106**, 86–88.

Kessler, H., Griesinger, C., Kerssebaum, R., Wagner, K. and Ernst, R.R. (1987) *J. Am. Chem. Soc.*, **109**, 607–609.

Kriwacki, R.W., Hill, R.B., Flanagan, J.M., Caradonna, J.P. and Prestegard, J.H. (1993) *J. Am. Chem. Soc.*, **115**, 8907–8911.

Leroy, J.L., Broseta, D. and Guéron, M. (1985) *J. Mol. Biol.*, **184**, 165–178.

Marion, D. and Wüthrich, K. (1983) *Biochem. Biophys. Res. Commun.*, **113**, 967–974.

Marion, D., Ikura, M., Tschudin, R. and Bax, A. (1989) *J. Magn. Reson.*, **85**, 393–399.

Mori, S., Johnson, M.O., Berg, J.M. and Van Zijl, P.C.M. (1994) *J. Am. Chem. Soc.*, **116**, 11982–11984.

Otting, G., Liepinsh, E. and Wüthrich, K. (1991a) *J. Am. Chem. Soc.*, **113**, 4363–4364.

Otting, G., Liepinsh, E. and Wüthrich, K. (1991b) *Science*, **254**, 974–980.

Otting, G., Liepinsh, E., Farmer II, B.T. and Wüthrich, K. (1991c) *J. Biomol. NMR*, **1**, 209–215.

Otting, G., Liepinsh, E. and Wüthrich, K. (1992) *J. Am. Chem. Soc.*, **114**, 7093–7095.

Otting, G. (1994) *J. Magn. Reson. Ser. B*, **103**, 288–291.

Otting, G. and Liepinsh, E. (1995) *J. Magn. Reson. Ser. B*, **107**, 192–196.

Piotto, M., Saudek, V. and Sklenář, V. (1992) *J. Biomol. NMR*, **2**, 661–665.

Qi, P.X., Urbauer, J.L., Fuentes, E.J., Leopold, M.F. and Wand, A.J. (1994) *Nature Struct. Biol.*, **1**, 378–381.

Sklenář, V., Tschudin, R. and Bax, A. (1987) *J. Magn. Reson.*, **75**, 352–357.